DISCRETE AND CONTINUOUS
DYNAMICAL SYSTEMS
Supplement 2011

Website: www.aimSciences.org

pp. **457–466**

PHASE-FIELD STUDY OF SOLUTE TRAPPING EFFECT IN RAPID SOLIDIFICATION

P.K. Galenko, E.V. Abramova and D.M. Herlach

Institut für Materialphysik im Weltraum,
DLR - Deutsches Zentrum für Luft- und Raumfahrt,
51170 Köln, Germany

Abstract. The phase-field model of Echebarria, Folch, Karma, and Plapp [Phys. Rev. E 70 (2004) 061604] is extended to the case of rapid solidification in which local non-equilibrium phenomena occur in the bulk phases and within the diffuse solid-liquid interface. Such an extension leads to the fully hyperbolic system of equations given by the atomic diffusion equation and the phase-field equation of motion. This model is applied to the problem of solute trapping, which is accompanied by the entrapment of solute atoms beyond chemical equilibrium by a rapidly moving interface. The model predicts the beginning of complete solute trapping and diffusionless solidification at a finite solidification velocity.

1. **Introduction.** The term "solute trapping" has been introduced to describe the process of non-equilibrium solute redistribution at the solid–liquid interface, which is accompanied by the entrapment of solute away from chemical equilibrium in solidification [1]. This process results in the deviation of the partition coefficient for solute distribution at the interface towards unity away from its equilibrium value, independently of the sign of the chemical potential [2].

The effect of solute trapping has been investigated theoretically using sharp-interface models [2] as well as using phase-field models [3, 4, 5, 6] of rapid solidification. In particular, solute trapping is characterized by the solute segregation coefficient $k(V)$, which is dependent on the interface velocity V, and is evaluated by the following ratio

$$k(V) = \left.\frac{\text{concentration in solid}}{\text{concentration in liquid}}\right|_{\text{interface}}. \tag{1}$$

This segregation coefficient $k(V)$ includes the kinetic parameter in a form of the solute diffusion speed V_D^I at the interface [2]. Quantitative analysis of such a function $k(V)$ shows reasonable agreement with experimental findings at small and moderate growth velocities of crystals. However, the results of natural experiments exhibit the complete solute trapping regime which occurs at $k(V) = 1$ at a finite interface velocity V which is not predicted by the function $k(V)$ including the solute diffusion speed V_D^I at the interface only. As it has been established [7], to describe increasing $k(V)$ up to $k(V) = 1$ at a finite V the model has to include both the finite speed V_D^I at the interface and the finite speed V_D^B of atomic diffusion in bulk phases.

2000 *Mathematics Subject Classification.* Primary: 80A22, 74D10; Secondary: 35L20.

Key words and phrases. hyperbolic equation, fast phase transition, phase-field model, rapid solidification, solute trapping.

The main scope of the present article is to develop a phase-field model for solute trapping in rapid solidification which takes into account both solute diffusion speeds within the diffuse interface and bulk phases. This development is given as an extension of the Echebarria-Folch-Karma-Plapp phase-field model (the EFKP-model) [8], which is previously developed to the case of diluted binary systems solidifying closely to thermodynamic equilibrium. Such extension leads to a model represented by a couple of partial differential equations of hyperbolic type. To predict the complete solute trapping observable in experiments and predicted by the sharp-interface model (see results and discussions in Refs. [7]), the fully hyperbolic model is analyzed, and the results compared with those of the parabolic phase-field model [8].

2. **The model.** Consider a system consisting of A-atoms (solvent) together with a tiny amount of solutal B-atoms (solute) under constant temperature T and constant pressure. The requirement that the free energy monotonically decreases during the relaxation of the entire system to equilibrium leads to the following equations [9, 10]

$$\tau_D \ddot{C} + \dot{C} = \nabla \cdot \left[M_C \left(f_{CC} \nabla C + f_{C\varphi} \nabla \varphi \right) \right], \tag{2}$$

$$\tau_\varphi \ddot{\varphi} + \dot{\varphi} = M_\varphi \left(\varepsilon_\varphi^2 \Delta \varphi - f_\varphi \right), \tag{3}$$

where τ_D is the relaxation time for the diffusion flux, M_C the mobility of B-atoms, τ_φ the time scale for the relaxation of the rate of change of the phase field $\dot{\varphi}$, and M_φ is the mobility of the phase field. Also, the following notation for derivatives are accepted: $\dot{C} \equiv \partial C/\partial t$, $\ddot{C} \equiv \partial^2 C/\partial t^2$, $f_C \equiv \partial f/\partial C$, $f_{C\varphi} \equiv \partial^2 f/\partial C \partial \varphi$, $f_{CC} \equiv \partial^2 f/\partial C^2$, $\ddot{\varphi} \equiv \partial^2 \varphi/\partial t^2$, $f_\varphi \equiv \partial f/\partial \varphi$.

Eqs. (2)-(3) represent a fully hyperbolic system of equations. It describes solidifying system in which the free energy does not increase in time and the atomic balance law is satisfied with the assumption of positive values of the mobility coefficients M_C and M_φ (for details, see [11]). The thermodynamic consistency of the system (2)-(3) is proved by the condition of positive entropy production and by outcomes of the fluctuation-dissipation theorem [9].

To complete the definition of the system (2)-(3), let us choose the concrete free energy density f under condition of local equilibrium. Following the EFKP-model, the local equilibrium free energy density f is chosen as the ideal solution of a dilute binary system [8]:

$$f(C,T,\varphi) = f^A(T_A) - (T - T_A)s(\varphi) + \epsilon(\varphi)C + \frac{RT}{v_m}\Big(C \ln C - C\Big) + W g(\varphi), \tag{4}$$

where f^A is the free energy density of a pure system consisting of a solvent (atoms of A-sort), T_A is the solidification temperature of the solvent, R is the gas constant, v_m the molar volume (assumed equal for A- and B-atoms), W the height of the energetic barrier which is modeled by the double-well function

$$g(\varphi) = \varphi^2 \left(1 - \varphi\right)^2. \tag{5}$$

The entropy density $s(\varphi)$ and the internal energy density $\epsilon(\varphi)$ (accepted as for a pure one-component system) are derived using the dilute alloy approximation [8]

$$s(\varphi) = \frac{s_s + s_l}{2} - p_s(\varphi)\frac{L}{2T_A}, \quad p_s(\varphi) = 1 - 2p(\varphi), \tag{6}$$

$$\epsilon(\varphi) = \frac{\epsilon_s + \epsilon_l}{2} - p_\epsilon(\varphi)\frac{RT}{2v_m}\ln k_e, \quad p_\epsilon(\varphi) = \frac{2}{\ln k_e}\ln\left[k_e + p(\varphi)(1 - k_e)\right] - 1, \tag{7}$$

where L is the latent heat of solidification, and indexes "l" and "s" are related to the liquid and solid phase, respectively. It is straightforward to show that, using a common tangent construction, the accepted dilute alloy approximation leads to straight lines of the solidus $T_S = T_A + m_e C/k_e$ and the liquidus $T_L = T_A + m_e C$ in the phase diagram with the equilibrium coefficient k_e for the B-atom partitioning and the tangent $m_e = -(1-k_e)(RT/v_m)(T_A/L)$ of the liquidus line.

The interpolation function $p(\varphi)$ is taken to be

$$p(\varphi) = 30\int_0^{\varphi} g(s)ds = 6\varphi^5 - 15\varphi^4 + 10\varphi^3 \tag{8}$$

with

$$1 - p(\varphi) = p(1-\varphi), \qquad p'(0) = p'(1) = p''(0) = p''(1) = 0. \tag{9}$$

The functions $g(\varphi)$ and $p(\varphi)$ (given by Eqs. (5) and (8), respectively) are a feature of the specific choice of phase-field model (see references and explanations in [10]). These functions define the liquid state for $\varphi = 1$ and the solid state for $\varphi = 0$.

3. **Numerical solution.**

3.1. **Parameters of the phase field and solute diffusion.** The present computations use the following model parameters (see Ref. [4] and references therein): - the gradient energy factor ε_φ^2, the energetic barrier height W, the capillary parameter d_0, and the mobility M_φ of the phase field expressed in terms of the surface energy σ, the interfacial width δ, and the field diffusion parameter ν:

$$\varepsilon_\varphi^2 = 2\sigma\delta, \qquad W = \frac{9\sigma}{\delta}, \qquad d_0 = \frac{\sigma v_m}{RT_A}, \qquad M_\varphi = \frac{\nu}{2\sigma\delta}, \tag{10}$$

- the diffusion coefficient of the B-atoms dissolved in A-solvent (i.e., interdiffusion coefficient in the accepted dilute alloy approximation) within the diffuse interface taking into account bulk diffusion coefficients D_L and D_S in the liquid and solid, respectively:

$$D(\varphi) = D_S + p(\varphi)(D_L - D_S), \tag{11}$$

- the atomic mobility:

$$M_C(T, C, \varphi) = \frac{D(\varphi)}{f_{CC}(T, C, \varphi)}. \tag{12}$$

Note that the phase field mobility from Eq. (10) is assumed to be positive at $\nu > 0$ and the atomic mobility (12) is positive at $f_{CC} > 0$. This guarantees monotonic behavior of the free energy with its non-positive dissipation in solidifying system [11].

TABLE 1. Analytical expressions and numerical values for the characteristic speeds of the atomic diffusion and the phase field propagation in the Si-As alloy

Parameter	Expression
Speed of solute diffusion within the diffuse interface	$V_D^I = D_L/\delta$=0.8 (m/s)
Scale of diffuse interface speed	$V_\varphi^I = \nu/\delta$=8.37 (m/s)
Speed of solute diffusion in bulk liquid	$V_D^B = (D_L/\tau_D)^{1/2}$=2.5 (m/s)
Maximum speed for phase field propagation	$V_\varphi^B = (\nu/\tau_\varphi)^{1/2}$=39.6 (m/s)

3.2. **Equations in the moving reference frame.** The solute trapping problem is analyzed in one spatial dimension with a planar interface using the model parameters (10)-(12). In this case, we use the following dimensionless co-ordinate reference frame, $x \to (x - Vt)/\delta$ and $t \to t\nu/\delta^2$, which is moving with the constant interface velocity V with the origin $x = 0$ placed at $\varphi = 1/2$. Then, the governing equations (2)-(3) can be written in the following dimensionless form:
- the concentration field

$$\frac{V^2}{(V_D^B)^2}\frac{\partial^2 C}{\partial x^2} - \frac{V}{V_D^I}\frac{\partial C}{\partial x} = \frac{\partial}{\partial x}\left(\hat{D}(\varphi)\frac{\partial C}{\partial x}\right) + \frac{\partial}{\partial x}\left(\hat{D}(\varphi)C\Theta(\varphi)\frac{\partial p(\varphi)}{\partial \varphi}\frac{\partial \varphi}{\partial x}\right), \quad (13)$$

- the phase field

$$\frac{V^2}{(V_\varphi^B)^2}\frac{\partial^2 \varphi}{\partial x^2} - \frac{V}{V_\varphi^I}\frac{\partial \varphi}{\partial x} = \frac{\partial^2 \varphi}{\partial x^2} - \frac{9}{2}\frac{\partial g}{\partial \varphi} + \frac{1}{2}\frac{\delta}{d_0}\frac{T}{T_A}\Lambda(T, C, \varphi)\frac{\partial p(\varphi)}{\partial \varphi}. \quad (14)$$

Eqs. (13)-(14) describe quasi-stationary phase-field dynamics in which, using contributions (5)-(9) to the free energy density (4), the following functions are introduced

$$\Theta(\varphi) = -\frac{1 - k_e}{k_e + (1 - k_e)p(\varphi)}, \quad (15)$$

$$\Lambda(T, C, \varphi) = -\frac{1 - k_e}{m_e}(T - T_A) + \frac{(1 - k_e)C}{k_e + (1 - k_e)p(\varphi)}, \quad (16)$$

and, using the definition (11), the dimensionless diffusion coefficient is

$$\hat{D}(\varphi) = D(\varphi)/D_L = D_S/D_L + p(\varphi)(1 - D_S/D_L). \quad (17)$$

Eqs. (13)-(14) include interfacial and bulk characteristic speeds defined and estimated in Table 1. Using these definitions, within the local equilibrium limits $\tau_D \to 0$ and $\tau_\varphi \to 0$, the bulk speeds become infinite $V_D^B \to \infty$ and $V_\varphi^B \to \infty$ and the system (13)-(14) transforms into the previously investigated case of solute trapping [4, 6] which takes into account local non-equilibrium effects within the diffuse interface only. Finally note that Eqs. (15) and (16) present contributions into the driving force for diffusion and driving force for interface motion, respectively. These are essentially differ from those obtained for the hyperbolic extension of the Wheeler-Boettinger-McFadden-model (the WBM-model) [10].

3.3. **Method of solution.** The numerical solution is obtained for the specific case of a Si-4.5 at.%As alloy with material parameters given in Ref. [10]. Taking the first integral from Eq. (13), we arrive at the following equation for solute diffusion

$$\bar{D}(\varphi)\frac{\partial C}{\partial x} + \Theta(\varphi)\hat{D}(\varphi)C\frac{\partial p(\varphi)}{\partial \varphi}\frac{\partial \varphi}{\partial x} + \frac{V}{V_D^I}(C - C_0) = 0. \quad (18)$$

In this equation, the dimensionless diffusion parameter

$$\bar{D}(\varphi) = \left(\hat{D}(\varphi) - (V/V_D^B)^2\right)\theta\left[\hat{D}(\varphi) - (V/V_D^B)^2\right] \quad (19)$$

is introduced with the Heaviside function

$$\theta[r] = \begin{cases} 1, & r > 0, \\ 0, & r \le 0. \end{cases} \quad (20)$$

The definition of parameter (19) takes into account the extremely fast propagation of the interface when $\hat{D}(\varphi) - (V/V_D^B)^2 < 0$. The latter inequality leads to the diffusion field instability and abnormal increase of computed values for concentrations which have no physical meaning. Physically this instability leads to the fact

that diffusion has no time to act in the rapidly crystallizing local bulk of the system in which the interface velocity V is equal or greater than the diffusion speed V_D^B in bulk liquid. Therefore, instead of the difference $\hat{D}(\varphi) - (V/V_D^B)^2$ appearing after the first integration of Eq. (13), we introduce the diffusion parameter (19) which exhibits suppression of the atomic diffusion when $\hat{D}(\varphi) - (V/V_D^B)^2 < 0$.

Eqs. (18)-(20) are solved numerically by the Runge-Kutta method simultaneously with the phase-field equation (14) resolved by the relaxation method as follows:

$$\frac{\partial\varphi}{\partial\eta} = \left[1 - \left(V/V_\varphi^B\right)^2\right]\frac{\partial^2\varphi}{\partial x^2} + \frac{V}{V_\varphi^I}\frac{\partial\varphi}{\partial x} - \left(\frac{9}{2}\frac{\partial g(\varphi)}{\partial\varphi} - \frac{1}{2}\frac{\delta}{d_0}\frac{T}{T_A}\Lambda(T,C,\varphi)\frac{\partial p(\varphi)}{\partial\varphi}\right). \tag{21}$$

Here η is the effective "relaxation time".

The origin $x_0 = 0$ of the moving reference frame is placed in the point $\varphi = 1/2$ of the diffuse interface, therefore, the temperature T is relaxed by

$$\frac{1}{T_A}\frac{\partial T}{\partial\eta} = \frac{1}{\eta_V}\frac{\partial x_0}{\partial\eta} + \frac{1}{\eta_X}x_0. \tag{22}$$

Here η_V and η_X are numeric parameters of relaxation. The first term on the right hand side of Eq. (22) gives a feedback from the temperature to the relative interface velocity in the moving reference frame to reach $\partial x_0/\partial\eta \to 0$. The second term on the right hand side of Eq. (22) "attracts" the moving interface to the point $\varphi = 1/2$ providing $x_0 \to 0$. In limiting cases $\partial\varphi/\partial\eta \to 0$ and $\partial T/\partial\eta \to 0$, one obtains the stationary profiles of $\varphi(x)$ and $C(x)$ in the moving reference frame.

Relaxation parameters η_V and η_X are used for optimizing the relaxation process. For a given interface velocity V, the relaxation takes about $10^5 \div 10^3$ iterations with the step $d\eta \approx 0.01$ of the "relaxation time" depending on the initial approximation and the value of V.

The initial condition for φ is taken as the diffuse step function $\varphi = 0.5[1 + \tanh\{3x/(2\delta)\}]$ and the temperature as $T < T_A$. Boundary conditions for the phase field are $\varphi(\infty) = 1$ and $\varphi(-\infty) = 0$.

Because Eq. (18) is a first order differential equation, it does not require specific boundary conditions for the concentration field. Therefore, we found the solution of Eqs. (18)-(20) for $\bar{D}(\varphi) > 0$ within the Cauchy problem. The special three cases (i) $(V/V_D^B)^2 < D_S/D_L$, (ii) $V/V_D^B > 1$, and (iii) $D_S/D_L \le (V/V_D^B)^2 \le 1$ are specified in the numerical solution as described in Ref. [10].

4. **Results of the modeling.** We consider the specific case of a Si-4.5 at.%As alloy with material parameters given in Ref. [10]. Numerical solutions for the parabolic EFKP-model [8] are obtained by solving Eqs. (18), (21), and (22) [together with Eqs. (11), (15)-(17)] with the local equilibrium limits $V_D^B \to \infty$ and $V_\varphi^B \to \infty$. The fully hyperbolic extension of the EFKP-model is given by the governing equations (18) and (21) [using Eqs. (15)-(17), the diffusion parameters (19)-(20), the temperature relaxation term (22), and the conditions of Section 3.3]. The predictions of the parabolic EFKP-model and its hyperbolic extension are compared for the obtained results of concentration fields (Fig. 1), the solute trapping by the solute segregation coefficient on a diffuse interface (Fig. 2), the "velocity - temperature" relationship (Fig. 3), and the kinetic phase diagrams (Fig. 4).

4.1. **Concentration profiles.** The change in the concentration profile (for atoms of As considered as a solute in the Si-4.5 at.%As alloy) as the interface velocity increases is shown in Fig. 1. It is seen that, as the velocity increases, the width

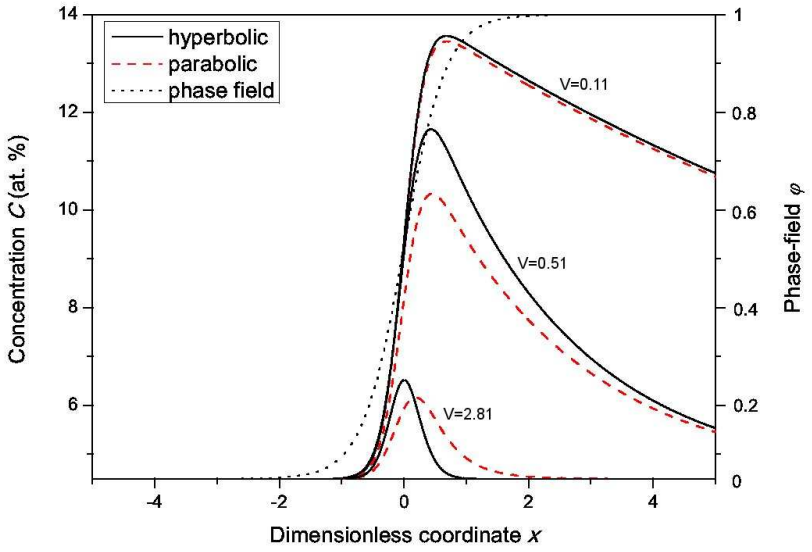

FIGURE 1. Concentration profiles for different interface velocities (indicated as "V" with dimensionality "m/s") and the phase-field profile. Calculations were carried out for Si-4.5 at.%As alloy and the constant interface width $\delta = 1.2 \cdot 10^{-9}$ m.

of concentration profile of the present hyperbolic extension of the EFKP-model shrinks faster than the parabolic EFKP-model. With the higher interface velocity, the small "hill" of the concentration profile is localized within the diffuse interface of the hyperbolic model (see profile at $V = 2.81$ m/s). Note that the position of the solute diffusion profiles at a given velocity depends on the chosen interfacial width δ. This dependence could be a subject of future modeling.

4.2. **Solute segregation.** In the context of a diffuse-interface description, solute segregation has been defined as the ratio of concentrations in the solid and at the maximum of concentration profile [4]. This definition has been analyzed and revised [6]. In particular, it has been suggested to take the ratio of concentrations at some distance from the "center" of the diffuse interface, which belongs to the solid and liquid phases from both sides of the interface. In the present work, to evaluate numerically the solute segregation coefficient (1), we take the definition

$$k(V) = \left(C|_{\varphi=0.001}\right) / \left(C|_{\varphi=0.999}\right), \tag{23}$$

which is consistent, in principle, with the one given in Ref. [6, 10]. Therefore, using the computed concentrations, in Fig. 1, the solute segregation coefficient is computed as a function of interface velocity V at the values of $\varphi = 0.001$ for the solid and $\varphi = 0.999$ for the liquid phase, which actually establish the boundaries of the diffuse interface.

As is shown in Fig. 2, the parabolic EFKP-model predicts a gradual increase of the non-equilibrium solute segregation coefficient $k(V)$ in the entire region of the

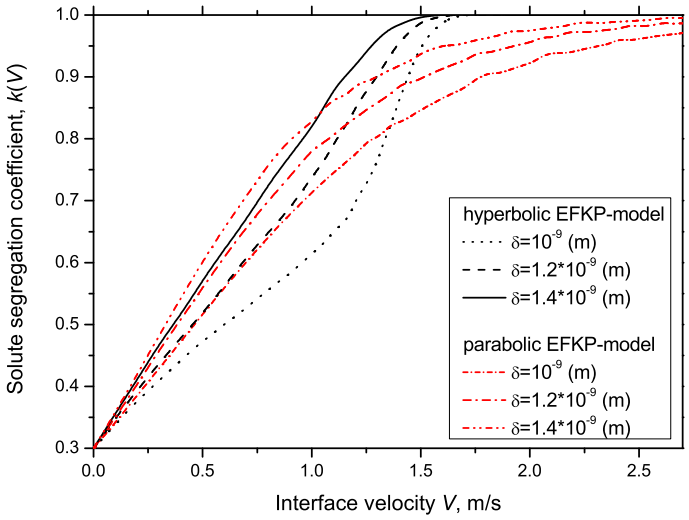

FIGURE 2. Non-equilibrium solute segregation coefficient $k(V)$ for Si-4.5 at.%As alloy. Results of the modeling are summarized for the parabolic EFKP-model, and its extension to the hyperbolic model, at various interfacial widths δ.

interface velocity V investigated. These results reproduce previous predictions obtained by the WBM-type models [4, 6]. By contrast, the hyperbolic model predicts a more abrupt change to the complete solute trapping, $k(V) \equiv 1$, at a fixed interface velocity as is clearly seen in Fig. 2. This result is qualitatively consistent with experimental findings, results of molecular dynamic simulations, and outcomes from the hyperbolic extension of the continuum growth model (see results and discussions in Refs. [7, 10]).

4.3. **Temperature and interface velocity.** The temperature T as a function of the interface velocity V differs substantially between both models. The gradual shrinking of the concentration profile and the gradual increase in the solute trapping function predicted by the parabolic EFKP-model (see Figs. 1 and 2) leads to a smooth and gradual behavior of the $T(V)$-function (see upper curves in Fig. 3). In contrast, the hyperbolic EFKP-model predicts non-monotonic behavior of the $T(V)$-function with a clear minimum in temperature at some value of the velocity. The minimum in the $T(V)$-function is consistent with the drastic shrinking of the solute diffusion profile up to the characteristic length $L_D = 2D[1 - (V^2/V_D^B)^2]/V$ comparable with the interface width.

Therefore, as predicted by the hyperbolic model (see the lower curves in Fig. 3), one can distinguish between:
- the regime with increasing undercooling to surmount the resistance of the developed solute atmosphere around the interface. This regime exists from the smallest interface velocity up to the interface velocity at which the $T(V)$-function is at minimum,
- the regime in which the system and, especially, the interface are heating up with

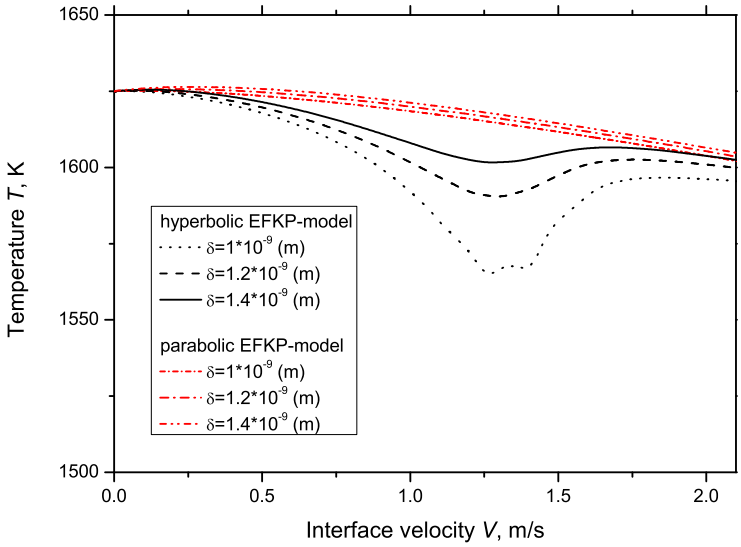

FIGURE 3. Dependence of temperature in the computational domain on interface velocity. Results for the parabolic EFKP-model and its extension to the hyperbolic model are shown for various solid-liquid interface width δ in solidifying Si-4.5 at.%As alloy.

a decrease of undercooling due to the absence of developed solute diffusion profile. This regime exists from the velocity giving the minimum of the $T(V)$-function up to highest velocity giving complete solute trapping.

4.4. **Kinetic phase diagrams.** Fig. 4 exhibits kinetic phase diagrams of the rapid solidification of the alloy in the coordinates "interface temperature - concentration" constructed using modeling results of the hyperbolic extension of the EFKP-model. We found that the actual interval of solidification, as a distance between lines of liquidus and solidus, shrinks with the increase of interface velocity V. This is clearly seen by comparing the solid lines for the equilibrium state with V=0 (m/s) and the dashed lines for kinetic liquidus and solidus lines for V=0.4 (m/s), shown in Fig. 4(a). With a higher interface velocity, $V \geq$1.5 (m/s), the kinetic liquidus and solidus lines merge into one line, shown as a dashed line in Fig. 4(b). This result indicates the equality of the solid and liquid concentrations on both sides of the diffuse interface: in the modeling we found

$$C|_{\varphi=0.001} = C|_{\varphi=0.999} \equiv \text{initial (nominal) alloy composition with } k(V) \equiv 1.$$

This result can be recognized as one of the main characteristics of complete solute trapping that accompanies diffusionless solidification.

Note that using the parabolic system of phase-field equations one can find that kinetic liquidus and solidus lines only gradually approach each other as the velocity V increases (see, e.g., kinetic diagram in Fig. 4 of Ref. [5]). Chemically partitionless solidification is also predicted previously using a sharp-interface model in which

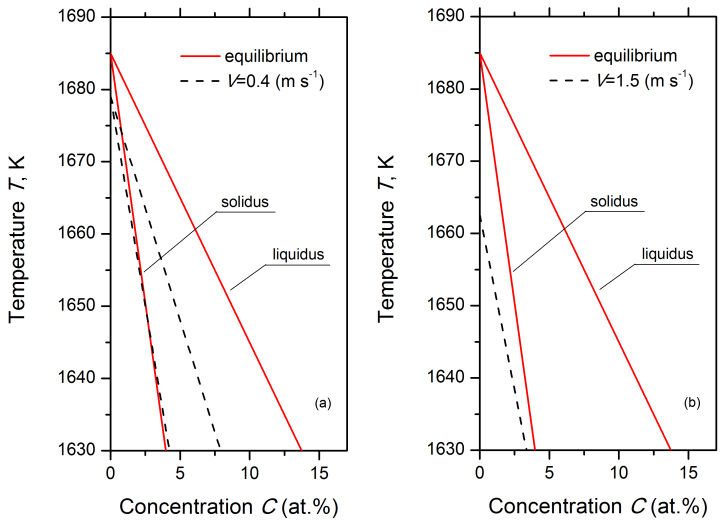

FIGURE 4. Kinetic phase diagram with the linear approximation of liquidus and solidus lines for Si-As alloys derived from the hyperbolic model. Computations are made for the interfacial width taken from Ref. [10]. Solid lines represent equilibrium lines of the liquidus and solidus. (a) Shift of the kinetic liquidus and solidus from their equilibrium positions at the interface velocity V =0.4 (m/s). Dashed lines give kinetic liquidus and solidus. (b) Confluence of the kinetic liquidus and solidus in one line as a result of the complete solute trapping and diffusionless solidification. Dotted line gives kinetic liquidus and solidus.

solute transport has been described by the hyperbolic equation (see, e.g., kinetic diagram in Fig. 4 of Ref. [12]).

5. **Conclusions.** The phase-field parabolic model of Echebarria, Folch, Karma, and Plapp (EFKP-model) [8] has been extended to the case of local non-equilibrium solidification. Four kinetic parameters were appearing in the model as main characteristics of local non-equilibrium effects. These are the characteristic speeds of atomic diffusion and phase field propagation within the moving diffuse solid-liquid interface and in bulk phases (see Table 1). The model is described by a system of hyperbolic partial differential equations for the atomic diffusion transport and diffuse interface advancement.

The present hyperbolic model is applied to the solute trapping problem. Modeling results have been analyzed by considering solute concentration profiles, the solute segregation coefficient, "temperature-velocity" relationships, and kinetic phase diagrams. A comparison with the predictions of the parabolic EFKP-model has shown that the present hyperbolic extension of EFKP-model predicts that complete solute trapping and diffusionless solidification begin at the fixed interface velocity at which the alloy solidifies as a supersaturated solid solution with the initial chemical

composition. However, as is shown in Figs. 2 and 4(b), the complete atomic trapping has begun in the present modeling at the critical interface velocity $V_c \approx 1.5(\mathrm{m/s})$ which is much smaller than the solute diffusion speed $V_D^B = 2.5(\mathrm{m/s})$ [see Table 1] at which the complete solute trapping should begin. The result at which the complete solute trapping begins at the smaller velocity (at $V_c < V_D^B$) than it is expected (with $V_c \geq V_D^B$) is also obtained using the hyperbolic WBM-phase-field-model [10]. We attribute this result to the definition of the segregation coefficient (23) which only gives asymptotical values for the ends of the diffuse interface in the non-equilibrium steady state interfacial motion. Therefore, with regard to obtaining the correct quantitative complete solute trapping, the $k(V)$-function has to be qualitatively redefined. This can be done in a future work.

Acknowledgments. We thank Denis Danilov and Vladimir Lebedev for fruitful discussions. P.K.G. and D.M.H acknowledge support from DFG (German Research Foundation) under the Project No. HE 160/19 and DLR Space Management under contract 50WM1140. E.V.A. acknowledges support from DAAD (German Academic Exchanges Service) under Stipendium A/08/81583 and RFBR (Russian Foundation of Basic Research) under Project 09-02-12110-ofi-m.

REFERENCES

[1] J.C. Baker, J.W. Cahn, *Solute trapping by rapid solidification*, Acta Metall., **17** (1969), 575–583.
[2] M.J. Aziz, T. Kaplan, *Continuous growth model for interface motion during alloy solidification*, Acta Metall., **36** (1988), 2335–2348.
[3] M. Conti, *Solute trapping in directional solidification at high speed: A one-dimensional study with the phase-field model*, Phys. Rev. E, **56** (1997), 3717–3720.
[4] N.A. Ahmad, A.A. Wheeler, W.J. Boettinger, G.B. McFadden, *Solute trapping and solute drag in a phase-field model of rapid solidification*, Phys. Rev. E, **58** (1998), 3436–3450.
[5] K. Glasner, *Solute trapping and the non-equilibrium phase diagram for solidification of binary alloys*, Physica D, **151** (2001), 253–270.
[6] D. Danilov, B. Nestler, *Phase-field modelling of solute trapping during rapid solidification of a Si-As alloy*, Acta Mater., **54** (2006), 4659–4664.
[7] P. Galenko, *Solute trapping and diffusionless solidification in a binary system*, Phys. Rev. E, **76** (2007), 031606-1-9.
[8] B. Echebarria, R. Folch, A. Karma, M. Plapp, *Quantitative phase-field model of alloy solidification*, Phys. Rev. E, **70** (2004), 061604-1-14.
[9] P. Galenko, D. Jou, *Diffuse-interface model for rapid phase transformations in nonequilibrium systems*, Phys. Rev. E, **71** (2005), 046125-1-13.
[10] V.G. Lebedev, E.V. Abramova, D.A. Danilov, P.K. Galenko, *Phase-field modeling of solute trapping: comparative analysis of parabolic and hyperbolic models*, International Journal of Materials Research, **101/04** (2010), 473–479.
[11] V. Lebedev, A. Sysoeva, and P.K. Galenko, Unconditionally gradient-stable computational schemes in problems of fast phase transitions, Phys. Rev. E, **83** (2011), 026705-1-11.
[12] P. Galenko, S. Sobolev, *Local nonequilibrium effect on undercooling in rapid solidification of alloys*, Phys. Rev. E, **55** (1997), 343–352.

Received July 2010; revised March 2011.

E-mail address: peter.galenko@dlr.de